

Parallel implementation of the algorithm for solving a problem of shock-wave accumulation in liquids*

V.D. Korneev, V.A. Vshivkov, G.G. Lazareva, V.K. Kedrinskii

Abstract. The new parallel algorithm has been developed and implemented for solving the axially symmetric problem of the interaction of a plane shock wave with a free bubble system (cluster) resulting in the formation of a stationary oscillating shock wave. The important characteristics of the problem in question, such as acceleration, effectiveness, the influence of inhomogeneities on the time of calculation were experimentally obtained, thus enabling evaluating of the quality of this algorithm as well as possibilities of obtaining good results. With the use of the parallel algorithm discussed, the dynamics of the pressure fields in a distant zone of a cluster is investigated, including the pressure field of the shock wave radiated by a bubble cluster. It is fairly difficult – during a reasonable time – to obtain results of such an investigation on one computer due to a large size of the problem under consideration.

1. Introduction

Generation of pressure pulses in liquids and gases has been the subject of ongoing research for many years. This work resulted in the development of various pressure generators and shock-wave accumulation methods. Research efforts were focused on the exploration of media in which the energy transferred by relatively weak pulsed loading can be absorbed, concentrated in a local region, and remitted in a pulse of a substantially higher amplitude. In the 1990s, the first publications appeared on the basic principles of hydroacoustic analogues of laser systems, such as SASER (shock amplification by systems with energy release) or SABSER (shock amplification by bubbly systems with energy release). In [1], the model developed by Iordanskii, Kogarko, and van Wijngaarden was used in numerical studies to show that interaction between a plane shock wave and a bubble cluster gives rise to a shock wave with a pressure gradient tangential to its curved front. By focusing such a wave, its amplitude can be increased by one or two orders of magnitude. Another example of waves in an axially symmetric geometry are the processes focusing in the interaction between a plane shock wave and a toroidal bubble cluster. The results of numerical study of the

*Supported by the Siberian Division of the Russian Academy of Sciences, Integration project No. 22.

near-axis wave structure was presented for a focusing shock wave emitted by a bubble cluster in [2]. It was shown that the wave reflected from the axis has an irregular structure. The Mach disk developing on the axis has a core of finite thickness with a non-uniform radial pressure distribution. The evolution of the Mach-disk kernel was analyzed, and the maximum pressure in the core was computed as a function of the gas volume fraction in the cluster. The effect of geometric parameters of the toroidal bubble cloud on the cumulative effect was examined.

This paper proposes the new parallel algorithm of the axially symmetric problem of the interaction of the plane shock wave with a free bubble system (the toroidal cluster) resulting in the formation in the liquid of a stationary oscillating shock wave.

The new approach to parallelization of the algorithm of the given problem is considered. The basic characteristics of the parallel algorithm, obtained for different sizes of a computer system, different sizes of a bubble cluster and different sizes of a problem are presented. The corresponding graphs of the numerical experiments are plotted. The results of solution to a concrete problem, obtained on the supercomputer system MVS100 are presented. The new results when solving the problem of the interaction of the plane shock wave with a toroidal cluster have been obtained. Analysis of the wave field structure in a distant zone of a cluster for three sets of geometrical parameters of the toroidal bubble cluster was made. The improved values of the pressure dynamics when the Mach disk is propagating along the axis for large time intervals have been obtained.

2. Statement of the problem and governing equations

We consider the shock wave generated by piston motion at the end of a shock tube of radius r_{st} filled with a liquid at the moment $t = 0$. The shock tube contains a toroidal bubble cluster whose center is located on the shock-tube axis (denoted by z) at a distance l_{cl} from its left boundary. The plane of

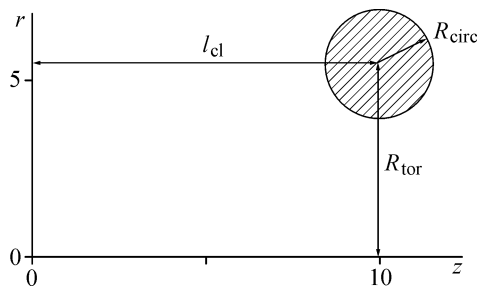


Figure 1. Toroidal bubble cluster: the hatched area is the toric section; z is the symmetry axis

of the base circle of the torus (hereinafter called the toric plane), which has a radius R_{tor} ($R_{tor} < r_{st}$), is perpendicular to the shock-tube axis. The cross-sectional radius of the torus is R_{circ} (Figure 1). The initial volume fraction of the gas phase in the cluster is denoted by k_0 . All gas bubbles have equal radii R_b , their distribution over a cluster being uniform. At $t > 0$, the shock wave propagates along

the positive axis z , interacts with a toroidal bubble cloud, bypassing around it, and is refracted as it encounters the cluster. The interaction between the refracted wave and the bubble cloud results in its focusing inside the cluster, and its intensity increases to an extent determined by the cluster parameters and the cross-sectional radius R_{circ} of the torus. The shock wave amplified by interaction with the cluster propagates further into the ambient liquid.

The focusing of the refracted wave by the cluster was computed using a modified Iordanskii–Kogarko–van Wijngaarden model [1], based on the continuity and momentum equations written down for the average pressure p , density ρ , and velocity \vec{u} :

$$\begin{aligned} \frac{\partial \rho}{\partial t} + \text{div}(\rho \vec{u}) &= 0, & \frac{\partial \vec{u}}{\partial t} + \vec{u}(\nabla \vec{u}) &= -\frac{1}{\rho} \nabla p, & (1) \\ p = p(\rho) &= 1 + \frac{\rho_0 c_0^2}{n p_0} \left[\left(\frac{\rho}{1-k} \right)^n - 1 \right], & k &= \frac{k_0}{1-k_0} \rho \beta^3, \end{aligned}$$

where ρ_0 is an unperturbed liquid density, c_0 is the speed of sound in a liquid, and ρ is the density of the bubble liquid normalized to ρ_0 . It is obvious that system (1) is not closed: the Tait equation of state for the liquid phase contains the volume fraction k of gas in the cluster, which is expressed in terms of the dynamic variable $\beta = R/R_0$ (a relative bubble radius).

In the Iordanskii–Kogarko–van Wijngaarden model, a physically heterogeneous medium is treated as homogeneous, and the Rayleigh equation for β :

$$\frac{\partial S}{\partial t} = -\frac{3}{2\beta} S^2 - \frac{C_1}{\beta^2} - C_2 \frac{S}{\beta^2} - \frac{p}{\beta} + \beta^{-3\gamma}, \quad (2)$$

where

$$S = \frac{\partial \beta}{\partial t}, \quad C_1 = \frac{2\sigma}{R_0 p_0}, \quad C_2 = \frac{4\mu}{R_0 \sqrt{p_0 \rho_0}},$$

is used as closure for system (1). Here σ is a surface tension, μ is viscosity, p_0 , ρ_0 , R_0 , $\sqrt{p_0/\rho_0}$, and $R_0 \sqrt{\rho_0/p_0}$, are the reference parameters used to obtain a dimensionless system of equations. In (1), $n = 7.15$.

In cylindrical coordinates, the flow domain is a rectangle with $0 \leq z \leq z_{\text{max}}$, $0 \leq r \leq r_{\text{st}}$. The boundary conditions set at $(z = 0)$ correspond to a steady shock wave of amplitude P_{sh} with prescribed axial velocity and zero radial velocity. Symmetry conditions are set at $r = 0$. The computations were performed for $k_0 = 0.001 \div 0.1$, $R_0 = 0.01 \div 0.4$ cm, and $P_{\text{sh}} = 3 \div 10$ MPa. The boundary condition set at $r = r_{\text{max}}$ rules out reflections of the shock wave from the shock-tube wall. For the wave emerging from the flow domain at $z = z_{\text{max}}$, the second axial derivatives of all variables are set to zero. To solve system (1), we adapted the upwind explicit and splitting schemes described in [3] to the present problem. At the first stage,

we applied the scheme proposed in [4]. Subsystem (2) was computed using the Runge–Kutta Merson fourth-order implicit scheme.

3. Parallelization of the algorithm of the problem solution

The computer system MVS1000 is a system with distributed memory. Such systems are primarily intended for computing the MPMD- and the SPMD-programming models. As is known, the problems that are solved by finite difference methods are efficiently parallelizable on computer systems with distributed memory with the use of the SPMD-model computation, or by the data decomposition method [5–11]. The latter is applied for parallelization of the algorithm of the problem in question.

According to the definition from Section 2, the computing model of the problem under consideration consists of a homogeneous liquid medium in a volume including a bubble cluster. Both media contribute differently to the total time of calculation, therefore, in order to elucidate features of a parallel algorithm, its characteristics are determined for different sizes of a computer system, different sizes of a cluster and different sizes of a problem.

3.1. The computational domain. A medium is set as a 2D rectangle of $X_m \times Y_m$ size (in centimeters). The bubble cluster is a 2D domain included into the medium of a given configuration.

In the domain of the medium, a uniform rectangular grid is set that defines a computational space with $N_m \times K_m$ nodes along the coordinates r and z . The same computational grid is used for the bubble cluster where applicable (Figure 2).

Values of each parameter that are calculated at the points of the given grid defining the medium and the bubble cluster are stored according to the number of parameters in 13 arrays, ten intended for the medium, and three—for the bubble cluster.

Three medium parameters and one parameter of the bubble cluster are calculated by the explicit five-point “cross” scheme. The other parameters make use of the values only at the same grid points, obtained at the $(k+1)$ th (previous) iterative step, when they are calculated at the grid points at the k th iterative step.

3.2. Parallelization of the algorithm. As stated above, the parallelization of the problem algorithm is carried out by the method of decomposition of computational spaces: the medium and the bubble cluster are divided into sub-domains, and these sub-domains are distributed at each node. The size and configuration of the sub-domains of the decomposed spaces are automatically calculated at each node according to their parameters and the value P that is equal to the number of nodes in a computer system. Decomposition of the medium and the bubble cluster spaces has some peculiarities.

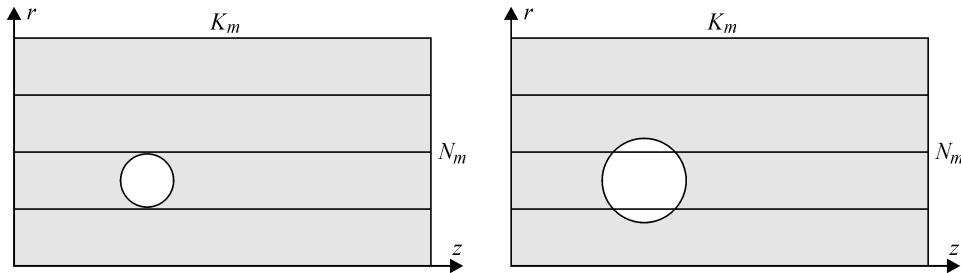


Figure 2. Examples of decomposition of computational sub-domains: a medium and a bubble cluster

Decomposition of the computational domain of the medium. The computational domain of the medium is divided into the equal strips along the coordinate z : $K_m/P \times N_m$, where P is the number of nodes, that is, the space is divided along the direction of the plane wave propagation (see Figure 2). Since the computational domain of the medium is represented by values of 10 parameters calculated at the grid points, then all the arrays are cut into sub-arrays, respectively. The arrays calculated by the “cross” scheme are decomposed with overlapping the values of the neighboring points of the boundary sub-domains. Decomposition of other arrays is done without overlapping the boundary sub-domains. All parts of the arrays corresponding to these sub-domains are then distributed among the nodes of the system.

Decomposition of the computational domain of the bubble cluster. The computational domain of the bubble cluster is divided similar to the medium space into strips along the coordinate z , the lines of cuts coinciding with those of the computational domain. The width of a strip in the computational domain depends on the number of processors P . As the computational domain of the cluster depends on the medium domain, the sizes of the sub-domains of the decomposed computational domain of the bubble cluster and their configuration for different P will be quite different (see Figure 2). The sub-domains of the decomposed cluster domain are distributed among nodes along with the respective sub-domains of the medium, to which the cluster is bound. Therefore, first the cluster sub-domains will be distributed not among all the nodes, and, second, the size and configuration of the cluster sub-domains distributed among the nodes will be different. The nodes among which the decomposed cluster sub-domains are distributed should be able to simulate these parts of the cluster in their memory. In this case, the simulation should be carried out automatically with different cuttings of this cluster. In the original sequential algorithm, the size of the bubble cluster, its configuration and location in the medium are set in a special manner, i.e., parametrically. The cluster sub-domains are determined at each node by the lines of cuttings of the computational domain. The decomposition

algorithm of the bubble domain is universal independent of the size and configuration of a cluster.

All the arrays of the parameter values defining the computational domain of the bubble cluster are cut to sub-arrays according to the partitioning of the domain. The array calculated by the “cross” scheme is decomposed with overlapping the values at the neighboring points of the boundary sub-domains. The other arrays are decomposed without overlapping the boundary sub-domains.

3.3. The computer system topology. The topology of a computer system, as is known, is defined by the structure of the algorithm of a problem in the case under consideration by the data structure, as the algorithm is parallelized by data. The data in the algorithm are divided into strips, and the data exchange in the course of calculation is only between the neighboring strips. Therefore, the linear topology of a computer system is sufficient for the problem solution. The strips of the decomposed computational domain of the medium are sequentially distributed among nodes following their numbers. The strip with the smallest coordinates of the grid points locates at the 0th node, the one with the bigger coordinates—at the 1st node, etc., the strip with the biggest grid coordinates—in the last node. The sub-domains of the bubble cluster are distributed among nodes according to the strips of the medium, where they are located.

The imposed boundary conditions of the computational domain of the medium along the coordinate z are located at the 0th and the last nodes, the boundary conditions along the coordinate r being located at all the nodes.

3.4. Acceleration and efficiency of the parallel algorithm. When developing a parallel algorithm, it is important to know of the possibilities to accelerate calculations as well as of overhead expenses associated with organization of the interactions of the parallel branches. In addition, it is important to know the efficiency coefficients, allowing its comparison with other parallel algorithms as well as evaluation of its quality from the standpoint of computational costs needed for the parallel interactions. Large volumes of data are required for obtaining a good result on the given problem. That is why, the characteristics of the parallel algorithm dependent on the size of a computer system allow us to estimate constraints of the problem size. Starting from this size, the efficiency and acceleration will either be zero or negative, and then we will have to find the new approaches to parallelization of the algorithm or to the problem solution as a whole.

The acceleration coefficient of a parallel algorithm on the computer system with $P > 1$ nodes (in the sequel, $P > 1$) according to [6] will be assessed by the value:

$$U_p = \frac{T_1}{T_p}, \quad (3)$$

where T_1 is the computational time of a sequential algorithm on one node; T_p is the computational time of a parallel algorithm on the computer system with P nodes.

The efficiency coefficient of a parallel algorithm on the computer system of P nodes will be assessed by the value:

$$F_p = \frac{T_{pc}}{T_{pc} + T_{pv} + T_{ps}}, \quad (4)$$

where T_{pc} is the computational time (other time costs not taken into account), T_{pv} are the total time costs per data exchanges between the nodes of the same system, T_{ps} is the total time costs needed for synchronization of branches of a parallel program.

The domain of the medium and the cluster domain differently affect the total time of calculations because of their differences in size and in the number of the major parameters. Therefore, for a better verification of the main characteristics of a parallel algorithm, let us consider two versions of testing:

- in the first version, the size of the cluster domain is fixed and the size of a computer system varies;
- in the second version, the size of a computer system is fixed, and the size of the cluster domain varies.

In the first version, testing is carried out for two different sizes of the medium domain.

3.5. Acceleration and efficiency of the parallel algorithm in calculations on different size systems. This section presents the results of the first version of testing the parallel algorithm of the problem under study. In this case, the characteristics of the algorithm are determined first for two different sizes of the medium domain, and, second, for the two types of calculations in each of these domains: 1) calculations in the medium with the cluster included in it and 2) calculations only in the homogeneous medium. In practice, the cluster domain can have an arbitrary configuration, that is why when calculating in the homogeneous medium without cluster, the characteristics of the parallel algorithm are limiting for the problem as a whole and, therefore, are interesting.

Here, also, one more coefficient is discussed, let us call it a relative acceleration

$$U_{p,2p} = \frac{T_p}{T_{2p}}.$$

This coefficient means the following: which value the algorithm acceleration will change for if the number of nodes in the system is twice increased.

Testing was carried out on the computer system MBC1000 on different number of nodes: on one, two, four, eight, 16 and 32 nodes with the use of the parallel programming system MPI [12, 13] and for the two sizes of medium domains. Let us denote them as O_1 and O_2 . In this case, O_1 was equal to $N_m \times K_m = 320 \times 3200$ grid points along the coordinates r and z , while O_2 was twice as large and was equal to $N_m \times K_m = 640 \times 3200$ grid points along the same coordinates. The cluster domain was the same for all the cases and represented a circle of $20 \cdot 10^3$ points.

Here the coefficients U_p , F_p , $U_{p,2p}$, and the total time of solving the problem T_p for calculations in a homogeneous medium O_1 will be denoted as U_p^1 , F_p^1 , $U_{p,2p}^1$, and T_p^1 , and for calculations with a cluster in the same medium — as \widehat{U}_p^1 , \widehat{F}_p^1 , $\widehat{U}_{p,2p}^1$, and \widehat{T}_p^1 .

In Figure 3, we present the comparison of coefficients U_p^1 , F_p^1 , and $U_{p,2p}^1$ with \widehat{U}_p^1 , \widehat{F}_p^1 , and $\widehat{U}_{p,2p}^1$, respectively, for the parallel algorithm when computing on a different number of nodes.

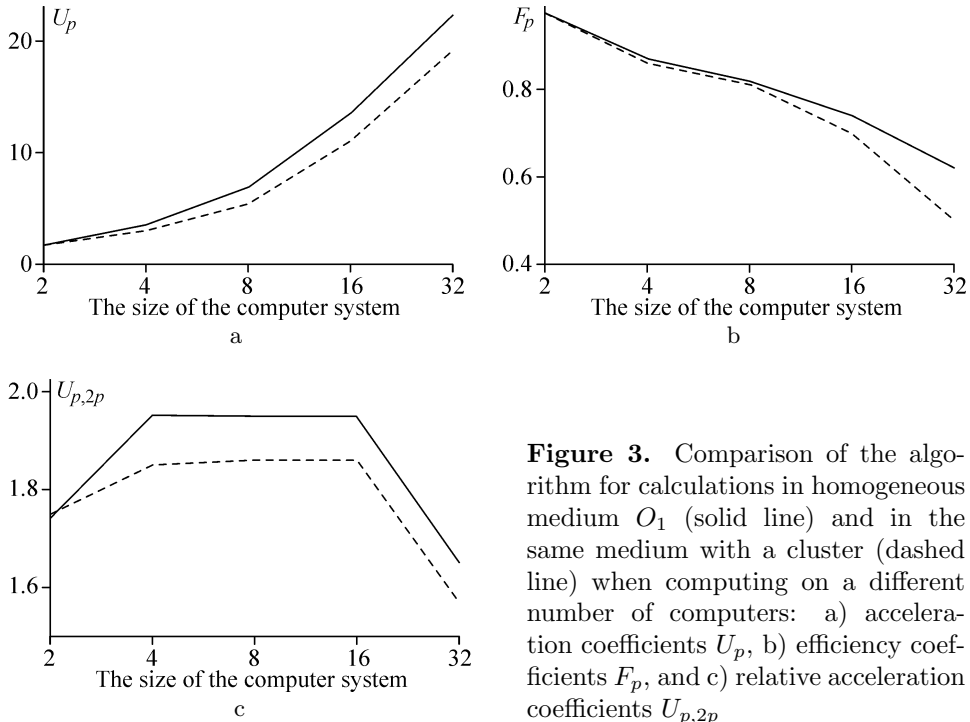


Figure 3. Comparison of the algorithm for calculations in homogeneous medium O_1 (solid line) and in the same medium with a cluster (dashed line) when computing on a different number of computers: a) acceleration coefficients U_p , b) efficiency coefficients F_p , and c) relative acceleration coefficients $U_{p,2p}$

In Figure 3a, the acceleration coefficients U_p^1 appeared to be sufficiently good, for example, $U_2^1 = 1.8$, $U_{32}^1 = 22$, i.e., on two nodes the speed of the algorithm was almost twice as large and on 32 nodes—twenty two times as large as compared to one node. When computing on P processors, each one takes P times less volume of the parallelized data. Thus, the total time of access to data is decreased on each node. Therefore, despite of the time losses associated with interaction of branches of the parallel program, the acceleration coefficients for a given size of a computer system are still good enough.

The coefficients U_p^1 are limiting for \widehat{U}_p^1 , i.e., the smaller the cluster domain, the closer the graphs \widehat{U}_p^1 to the graphs U_p^1 .

Acceleration coefficients of both types of calculations in the medium O_2 are close to those in the medium O_1 . Recall that O_2 is twice as large as O_1 .

In Figure 3b, the efficiency coefficients assess a “contribution” of overhead expenses to the total time of calculation with interactions between branches. It is evident that with an increase of sizes of a computer system the efficiency of parallel calculations gradually decreases. For systems consisting of two and more nodes, the communication channels between them essentially affect the speed of data exchange and, consequently, the total time of calculations. From (4), it follows that this graph shows a relative increase in the overheads needed for parallel interactions with the growth of the size of the computer system.

Let us note that graphs of the efficiency coefficients of the algorithm for calculations in the medium O_2 , like the acceleration coefficients in Figure 3a, are similar to the graphs, presented in Figure 3b.

The graphs of the relative acceleration coefficients $U_{p,2p}$ for different types of calculations (see Figure 3c) are also indicative and help in answering the question: how many times does the speed of calculation increase if a computer system is twice increased? One can see that if there are 32 nodes in a system instead of 16, then the acceleration $U_{p,2p}^1$ has increased only by coefficient 1.65, while $\widehat{U}_{p,2p}^1$ —only by coefficient 1.57. These graphs indicate to a decrease in the speed of calculations with an increase of the size of a computer system. This implies that with a certain size of a computer system, the growth of speed of calculation will be equal to 1 or even be negative. This is valid for a certain size of a problem.

The two latter graphs indicate to a decrease in efficiency as well as in a relative speed of calculations with a growth of a computer system. This should be so for a given type of a problem. For a concrete problem, with a growth of a computer system, the volume of data, distributed among each processor, decreases proportional to the size of this system (see Subsection 3.2). This means that the number of calculation operations decreases with a growth of the size of a computer system, while the number of exchange

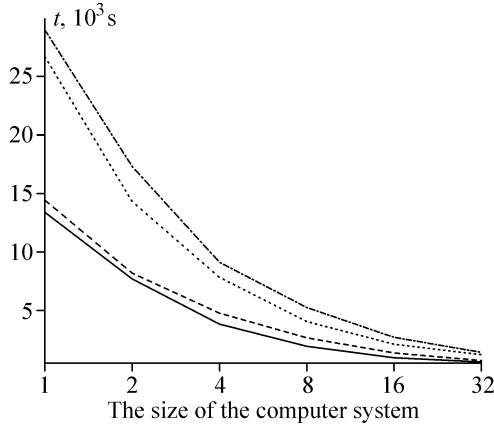


Figure 4. Graphs for the total computing time of the algorithm when computing on a different number of computers for calculations in the homogeneous medium O_1 (solid line), the medium O_1 with a cluster (dashed line), the homogeneous medium O_2 (dotted line), and the medium O_2 with a cluster (dash-dotted line)

operations—between parallel branches—remains the same. Here we mean the exchanges for calculations of three parameters of a medium and one cluster parameter (see Subsection 3.1). It should be noted here that graphs of the relative acceleration coefficients of the algorithm for calculations in the medium O_2 are similar to the graphs in Figure 3c.

And, finally, Figure 4 reflects the dependence of the total time of calculation on the size of a computer system for media of different sizes.

3.6. About the influence of the size of a bubble cluster on total time of parallel computation. In this section, we present the results of the second version of testing the parallel algorithm of the problem under study in the case when the size of a computer system is fixed and the size of the cluster domain varies.

For the problem in question, of no less importance is to know about the influence of the size of a bubble cluster on the total time of parallel computation. The testing was carried out on the computer system MVS1000 with a fixed number of nodes, i.e., four, but with different sizes of a cluster. In all the cases, the medium domain was the same and equal to $N_m \times K_m = 1280 \times 1280$ grid points along both coordinates. The size of a bubble cluster and its distribution among the nodes varied.

Two sub-versions were considered that are distinct both in size of clusters and in their location in the nodes. Inside each sub-version, the clusters differed only in size, their location in the nodes being the same. In this case, the size of a cluster was determined by the number of points of the cluster domain; its configuration being unimportant. In the first version, four clusters were considered with the sizes $K_1 = 50 \cdot 10^3$, $K_2 = 100 \cdot 10^3$, $K_3 = 150 \cdot 10^3$, and $K_4 = 200 \cdot 10^3$ points, respectively; in the second version there were also four clusters with $K_1 = 100 \cdot 10^3$, $K_2 = 200 \cdot 10^3$, $K_3 = 300 \cdot 10^3$ and $K_4 = 400 \cdot 10^3$ points. In the first version, clusters were

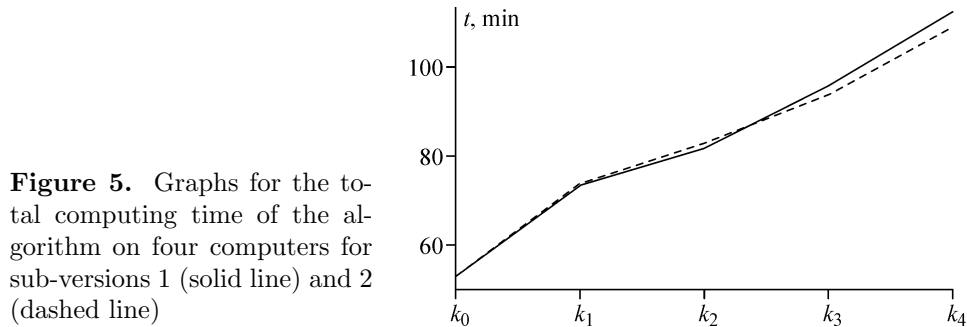


Figure 5. Graphs for the total computing time of the algorithm on four computers for sub-versions 1 (solid line) and 2 (dashed line)

located in one node, in the second version clusters were located in two nodes but with a uniform distribution of points among these nodes.

In both versions, comparisons were made both with parallel computations in a homogeneous medium (without cluster) and with calculations in a homogeneous medium of a sequential algorithm in one node.

In Figure 5, a graph of the times of parallel computations for both sub-versions of tests, obtained on the computer system consisting of four nodes is shown. Here k_0 denotes the time of calculation in a homogeneous medium without cluster, k_i ($i = 1, 2, 3, 4$) is the time of calculation in the medium with the corresponding cluster K_i for both sub-versions 1 and 2 (the notation of clusters is presented above).

These two graphs show that the size of a bubble cluster essentially affects the total time of calculating the problem. It should be mentioned that these graphs are almost equivalent. This is explained by the following. When a cluster is located only in one node, the time of calculation in it increases, while all other nodes have to wait for synchronization in exchanges on completion of cycles. If at this very time another node carries out the same task, the time delays will be the same.

4. Results of the parallel version testing

Figures 6–9 show distributed pressures in the plane (r, z) in a focusing shock wave generated by the toroidal bubble cloud at several instants. The pressure is quantified (in units of the hydrostatic pressure $p_0 = 0.1$ MPa). The maps were computed for $p_{sh} = 3$ NPa, $r_{st} = 40$ cm, $z_{max} = 65$ cm, $l_{cl} = 20$ cm, $k_0 = 0.01$, and $R_b = 0.1$ cm.

Let us dwell on three calculations with different geometrical parameters of a toroidal cloud of bubbles. As was shown in [2], the wave picture is defined not only by the volume of a bubble domain, but also by its shape. Let us compare the calculation results for a torus radius $R_{tor} = 6$ cm, radii of cross-sections $R_{circ} = 1$ cm and 6 cm (see Figures 6–8).

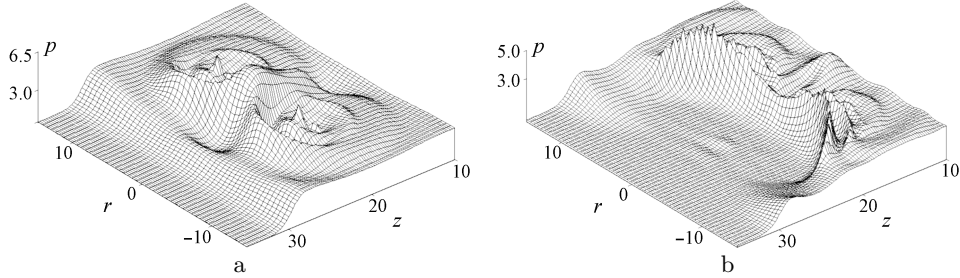


Figure 6. The pressure distribution after 200 μs for the values of parameters $R_{\text{tor}} = 6$ cm, $R_{\text{circ}} = 1$ cm (a) and 6 cm (b)

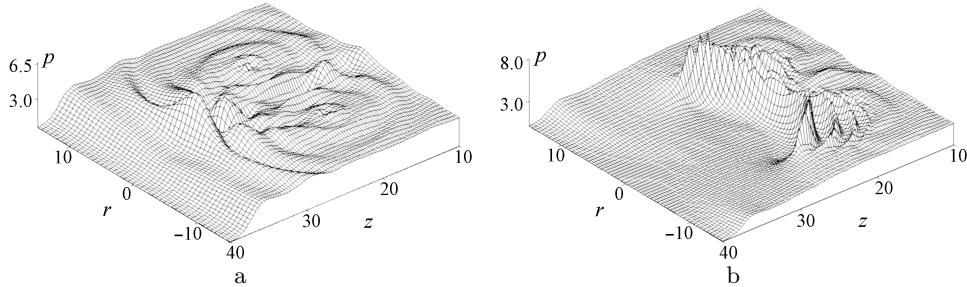


Figure 7. The same as in Figure 6, but after 250 μs

Figure 6 represents distributed pressures in the plane (r, z) after 200 μs . Despite of the fact that bubble clouds in the shock tunnel are located in the same place in all versions of calculations, the wave picture is specific in each case. In the first case (Figure 6a), the shock wave, radiated by the cluster, forms a domain of axially symmetric irregular reflection on the axis of the domain after 200 μs . In the second case, when the inner boundary of the torus is a point, the process of absorbing the energy of the incident shock wave by the cluster still takes place after the indicated time.

Figure 7 illustrates the pressure distribution after 250 μs . The results of calculations for the bubble cluster with a cross-section radius 1 cm (Figure 7a) demonstrate the formation of Mach disks on the axis of symmetry, while Figure 7b shows the shock wave, radiated by the toroidal bubble cloud, converging to the axis of symmetry.

After the time of 300 μs (see Figure 8), one can observe the radiation into the liquid of a sequence of spherical shock waves of low amplitudes. Such a radiation is generated by the cluster of the cross-section radius of 1 cm. In this case, the shock wave, radiated into the liquid by the cluster, is propagating along the axis and has the pressure amplitude 1.5 times as large as that of the wave falling on the bubble cloud at a distance of 20 cm from the torus plane. At that very time, the wave radiation by the cluster

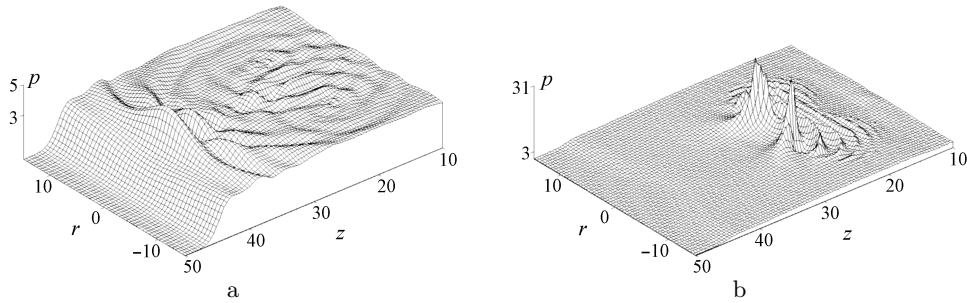


Figure 8. The same as in Figure 6, but after 300 μs

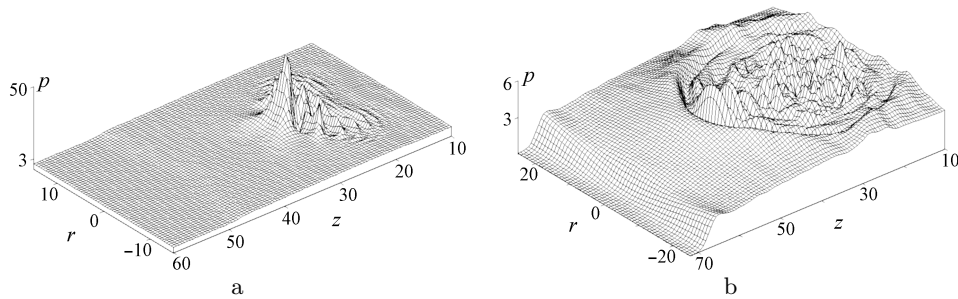


Figure 9. The pressure distribution for the values of parameters $R_{\text{tor}} = 6$ cm, $R_{\text{circ}} = 6$ cm after the time instants 320 (a) and 450 μs (b)

of the cross-section radius of 6 cm has just begun. In this case, the wave picture of the process of the radiated shock wave converging to the axis is quite different. The investigation of this process has become possible due to the use of multi-processor systems.

Figure 9 presents pictures of the distributed pressures for the values of parameters: $R_{\text{tor}} = 6$ cm, $R_{\text{circ}} = 6$ cm after the times of 320 and 450 μs . In this case, the topology of the current is the following: with such a configuration of a source, the front of the radiated shock wave, converging to the axis, represents a concave surface with a pressure gradient directed from the axis of symmetry. Despite of the fact that the pressure in the axis vicinity is minimal on the converging front, the accumulation of the current, in the end, results in the formation of a powerful solitary shock wave in the zone near to the source. This wave amplitude almost 30 times exceeds that of the wave interacting with the torus (Figure 9a). In the sequel, a chain of the Mach disks is formed on the axis (Figure 9b). The pressure amplitude in the irregular reflection zones is characterized by its large values, which essentially exceed the amplitudes of the spherical wave, radiated by the cluster into the liquid.

h	τ	Pressure		
		$R_{\text{tor}} = 6 \text{ cm}$ $R_{\text{circ}} = 1 \text{ cm}$	$R_{\text{tor}} = 1 \text{ cm}$ $R_{\text{circ}} = 1 \text{ cm}$	$R_{\text{tor}} = 6 \text{ cm}$ $R_{\text{circ}} = 6 \text{ cm}$
0.1000	0.000200	8.54	19.44	49.86
0.0500	0.000100	9.94	22.90	22.90
0.0125	0.000025	12.71	30.87	105.85

The character of the pressure amplitude distribution along the axis of symmetry is practically the same as in [2]. The use of supercomputers has allowed us to improve the earlier obtained results. The table presents the values of pressure for the calculation on a personal computer (lines 1, 2) and the same on the multi-processor system (line 3). As is seen, a maximum value of the pressure amplitude in the Mach disk kernel, obtained on the supercomputer is approximately 1/3 times as large as the one obtained on a single computer. The pressure amplitude in the Mach disk kernel is to a greater extent dependent on the geometrical cluster parameters than on the volume of the bubble cloud [2]. Let us compare maximum values of pressure in the Mach disk kernel shown in the table. The last column presents the calculation data for a bubble cluster with the parameters: $R_{\text{tor}} = 6 \text{ cm}$, $R_{\text{circ}} = 6 \text{ cm}$. For such a geometrical configuration of the toroidal cluster, the pressures in the Mach disk kernel are 35 times as large as the amplitude of the wave interacting with the torus. Thus, the pressure becomes eight times greater than in the case of the plane shock wave of the cluster with the parameters: $R_{\text{tor}} = 6 \text{ cm}$, $R_{\text{circ}} = 1 \text{ cm}$. As this takes place, the volume of the cluster is only six times as large. Let us consider the case when the toroidal cluster has the parameters: $R_{\text{tor}} = 1 \text{ cm}$, $R_{\text{circ}} = 1 \text{ cm}$. Hence, its volume is six times less than that of the cluster with the parameters: $R_{\text{tor}} = 6 \text{ cm}$, $R_{\text{circ}} = 1 \text{ cm}$. Nevertheless, the amplification obtained is 2.5 times higher.

Analysis of the wave field structure has shown [2] that as the Mach disk propagates along the axis, the pressure dynamics on the axis appears to be a non-monotonic function of a distance from the torus. With fixed parameters of the current, the pressure distribution has a distinct maximum, whose value is generally defined by the geometrical parameters of the toroidal bubble cluster (Figure 10). With an increase of a distance from the torus, a sharp growth of the pressure in the Mach disk kernel in its near zone is observed, the wave amplitude increasing by the factor of 4–35. In the case, when the inner torus boundary is a point, a sharp growth of pressure in the Mach disk kernel changes for a sharp decay. The character of the subsequent behavior of pressure indicates to an asymptotic tendency, when the pressures in the Mach disk kernels (at a distance of 20 cm from the torus) become practically equal. However these pressures still noticeably

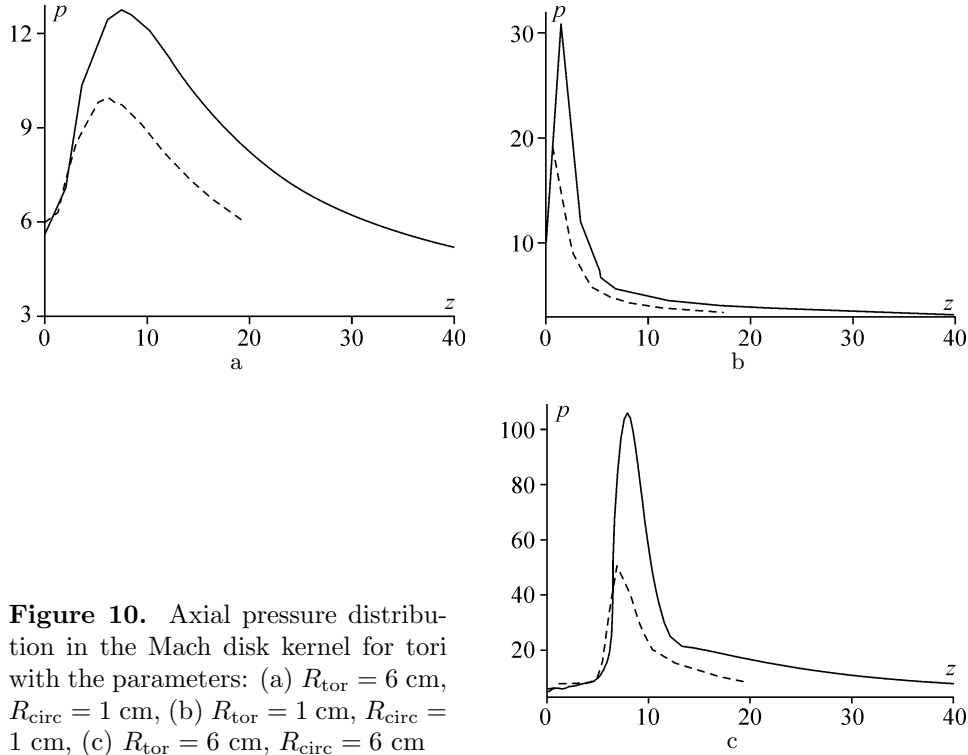


Figure 10. Axial pressure distribution in the Mach disk kernel for tori with the parameters: (a) $R_{\text{tor}} = 6$ cm, $R_{\text{circ}} = 1$ cm, (b) $R_{\text{tor}} = 1$ cm, $R_{\text{circ}} = 1$ cm, (c) $R_{\text{tor}} = 6$ cm, $R_{\text{circ}} = 6$ cm

exceed the amplitude of the wave interacting with the torus. Graphs show the pressure dynamics on the axis as function of distance from the torus. These graphs were plotted with the help of the sequential algorithm (dashed curves) and the parallel algorithm (solid curves). These graphs show three configurations of the bubble cluster. Calculations with the use of the parallel algorithm make it possible not only to define more precisely the pressure values in the Mach disk kernel, but, also, to obtain the pressure dynamics data on the axis in the far zone of the cluster. Obtaining high values of the pressure amplitude at large distances from a source is a challenging problem in acoustics. At a distance of 40 cm from the torus plane, the pressures in the Mach disk kernels exceed the amplitude of the wave, interacting with the torus by the factor of 1.5 ($R_{\text{tor}} = 6$ cm, $R_{\text{circ}} = 1$ cm) and by the factor of 2.5 ($R_{\text{tor}} = 6$ cm, $R_{\text{circ}} = 6$ cm). Thus, based on the data obtained, we may conclude that the case when the torus radii and the torus section are equal—this is the best effective configuration of the toroidal bubble cluster for attaining the directed radiation of a maximum amplitude. As is seen from Figure 10, maximum pressure values in the Mach disk kernel on the axis of symmetry of the torus are attained in a pure liquid. For example, the peak of pressure in the Mach disk kernel in the cluster with the parameters $R_{\text{tor}} = 6$ cm, $R_{\text{circ}} = 6$ cm is at a distance of 8 cm from the torus.

It is seen from the figures that calculations carried out on the supercomputer are more accurate and characterized by a wider scope of data to be obtained.

5. Conclusion

This paper proposes the new parallel algorithm of the axially symmetric problem of the interaction of the plane shock wave with a free bubble system (the toroidal cluster) resulting in the formation in the liquid of a stationary oscillating shock wave. The tests have shown that:

- the algorithm of the problem is parallelized sufficiently well on computer systems with distributed memory (if the medium domain is 320×3200 and the cluster domain has $20 \cdot 10^3$ points, we attain 22 times acceleration on 32 computers;
- Characteristics of the parallel algorithm do not become worse with an increase in the size of the problem;
- the new results were obtained when solving a real problem: the wave field structure in a distant cluster zone was analyzed for a wide range of geometrical parameters of a toroidal bubble cluster, the improved values of the pressure dynamics when the Mach disk is propagating along the axis were obtained for large time intervals.

It should be noted that each dimension of the problem in question corresponds to a certain size of a computer system that is optimal for solving this problem.

References

- [1] Kedrinskii V.K., Shokin Yu.I., Vshivkov V.A., et al. // *Docl. Akad. Nauk.* — 2001. — Vol. 381, No. 773 [*Docl. Phys.* — 2001. — Vol. 46, No. 856].
- [2] Kedrinskii V.K., Vshivkov V.A., Dudnikova G.I., et al. // *J. Experim. and Theor. Phys.* — 2004. — Vol. 125, No. 6. — P. 1302–1310.
- [3] Kovenya V.M., Lebedev A.S. // *Zh. Vychisl. Mat. Mat. Fiz.* — 1994. — Vol. 34, No. 886.
- [4] Kovenya V.M. // *Vychisl. Tekhnol.* — 1992. — Vol. 7, No. 59.
- [5] Evreinov E.V., Kosarev Yu.G. *High Efficiency Homogeneous Universal Computing Systems.* — Novosibirsk: Nauka, 1966.
- [6] Mirenkov N.N. *Parallel Programming for Multimodular Computing Systems.* — Moscow: Radio i Svyaz, 1989.

- [7] Korneev V.D. A system and methods of programming of multicomputers on an example of the computer complex PowrXplorer. — Novosibirsk, 1998. — (Preprint / Russ. Acad. Sci. Sib. Branch. Inst. Comp. Math. and Math. Geoph; 1123).
- [8] Korneev V.D. Parallel algorithms deciding the task of linear algebra. — Novosibirsk, 1998. — (Preprint / Russ. Acad. Sci. Sib. Branch. Inst. Comp. Math. and Math. Geoph; 1124).
- [9] Korneev V.D. Parallel Programming in MPI. — Novosibirsk: Russ. Acad. Sci. Sib. Branch, 2002.
- [10] Malyshkin V.E. Linearization of mass calculations. // System Computer Science / Ed. V.E. Kotov. — Novosibirsk: Nauka, 1991. — No. 1. — P. 229–259.
- [11] Malyshkin V.E., Vshivkov V.A., Kraeva M.A. About realization of the method of particles on multiprocessors. — Novosibirsk, 1995. — (Preprint / Russ. Acad. Sci. Sib. Branch. Comp. Center; 1052).
- [12] Snir M., Otto S.W., Huss-Lederman S., Walker D., Dongarra J. MPI: The Complete Reference. — Boston: MIT Press, 1996.
- [13] Dongarra J., Otto S.W., Snir M., Walker D. An introduction to the MPI standard. — 1995. — January. — (Tech. Report / University of Tennessee; CS-95-274).

